Clays and Clay Minerals, Vol. 44, No. 3, 357–369, 1996.

DICKITE, NACRITE AND POSSIBLE DICKITE/NACRITE MIXED-LAYERS FROM THE BETIC CORDILLERAS (SPAIN)

M. D. RUIZ CRUZ

Departamento de Química Inorgánica, Cristalografía y Mineralogía. Facultad de Ciencias.
Universidad de Málaga (Spain)

Abstract—Nacrite, dickite and intermediate dickite-nacrite phases have been identified from the upper Paleozoic sequences of the Maláguide Complex (Betic Cordilleras, Spain). Nacrite developed as euhedral, pseudohexagonal or elongated crystals within sandstones and thin, irregular veins. Dickite developed preferently within extensive zones of fractures as very irregular, compact packets. Intermediate phases occurred in the sandstones and veins similar to the nacrite, or accompanying dickite. The mineral assemblage of the sandstones includes quartz-muscovite-kaolinite-type minerals, with or without albite, carbonates, chlorite and mixed-layers containing chlorite. The metamorphic conditions in which these minerals formed belong to anchizone, as can be deduced from the IC values. Dickite, nacrite and intermediate phases were studied by X-ray diffraction, infrared spectroscopy, differential thermal analysis and microscopy. The results for dickite indicate a well-ordered mineral and agree with most of the published data. Conversely, IR spectra and DTA curves of nacrite show some differences in relation to the available data for this mineral. Based on the comparison with dickite and nacrite data, intermediate phases can be interpreted either as disordered varieties or as mixed-layered dickite/nacrite.

Key Words—Dickite, Differential thermal analysis, Infrared spectroscopy, Mixed-layers, Nacrite, Very low-grade metamorphism, X-ray powder diffraction.

INTRODUCTION

In recent papers (Ruiz Cruz and Moreno Real 1993; Ruiz Cruz 1996a, 1996b) the abundance of dickite within the Permo-Triassic materials of the Maláguide Complex (Internal zones of the Betic Cordilleras, Spain) has been pointed out. Study of the underlying Paleozoic has revealed the simultaneous presence of dickite, nacrite and intermediate phases in the upper Paleozoic (Carboniferous strata).

The presence of dickite during advanced diagenesis is well documented (Ferrero and Kubler 1964; Dunoyer de Segonzac 1970; Frey 1987). Nacrite, the rarest polytype of the kaolinite group, has been classically regarded as hydrothermal in origin (Deer et al. 1976), but its formation during advanced diagenesis and incipient metamorphism has also been described (Shutov et al. 1970). The difficulty of polytype determination by classical X-ray diffraction (XRD) methods is probably the reason for the limited information on the occurrence of nacrite. As pointed out by several other authors (Hanson et al. 1981; Wilson 1987; Shen et al. 1994), much that is described in the literature as kaolinite or dickite may actually be nacrite.

The identification of dickite and nacrite is usually based on the combined use of XRD and infrared spectroscopy (IRS). There is no difficulty in identifying these polytypes by XRD when they occur as pure minerals. For mixtures of these polytypes, and even with kaolinite, the presence of nacrite is indicated by the notable intensity decrease of the 2.50 Å and 2.32 Å reflections. Nacrite can be unambigously identified after treatment with potassium acetate and washing with water (Wada 1965) because the spacing of the resulting nacrite complex (at 8.40 Å) is clearly separated from those of kaolinite and dickite. Shutov et al. (1970) identified "mixed-packets" of dickite/nacrite from optical and electron microscope studies, which show reflections of both minerals, but cannot be explained as mixtures of them. The work of Shutov et al. (1970) constitutes the only clear reference to the possible dickite/nacrite interstratification.

Identification of dickite and nacrite by IRS is based on the position and relative intensity of the OH-stretching bands in the 3700 to 3600 cm^{-1} region, reported by Farmer (1974), Van der Marel and Beutelspacher (1976) and Russell (1987). According to these authors, the OH-stretching bands in nacrite occur at 3703-10, 3646-48 and 3628-30 cm^{-1} while those in dickite appear at about 3705, 3655 and 3620 cm^{-1}. In multicomponent mixtures, the identification of different polytypes becomes very difficult.

Differential thermal analysis (DTA) curves of dickite show a characteristic endotherm at 680 to 700 °C and an exotherm at about 1000 °C (Mackenzie 1970). The available DTA curves of nacrite (Mackenzie 1970; Hanson et al. 1981) are characterized by an endotherm at about 680 °C, intermediate between those of well-crystallized kaolinite and dickite, and by an exotherm at 1000 °C. Unfortunately, Shutov et al. (1970) does not offer DTA curves of nacrite or "mixed-packets" of dickite/nacrite.

In the present study, we report the transition of dickite to nacrite, unusual for metamorphic materials, and we offer new IRS and DTA data for nacrite. The nature of the intermediate phases, which can be interpreted as either disordered varieties or as mixed-layer dickite/nacrite is also discussed.

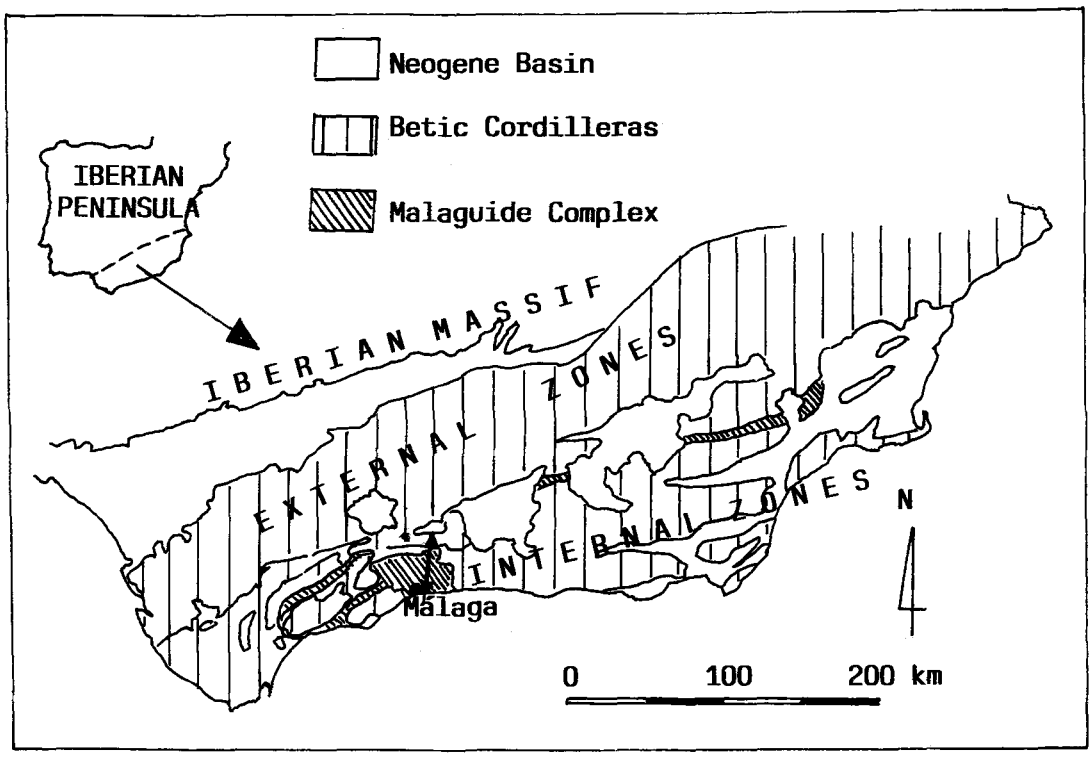

Figure 1. Position of the Maláguide Complex in the Betic Cordilleras and location of the studied area.

MATERIALS AND METHODS

The samples are from a thick section of Paleozoic strata situated within the Malaga zone (Southern Spain), which belongs to the Malaguide Complex of the Betic Cordilleras (Figure 1). Detailed descriptions of the Malaguide sequence are in numerous publications (Felder 1978; Mäkel 1985; Bourgois 1978).

The study of about 80 samples from a Silurian to Carboniferous sequence revealed the abundance of kaolinite-type minerals from the upper Paleozoic. A detailed sampling was carried out on 100 m of the Carboniferous sequence that showed the highest content on these types of minerals. The samples include several types of veins and fracture fillings, sandstones and fine-grained sediments, all altered by very low-grade metamorphism.

Whole rock samples were analyzed by XRD, scanning electron microscopy (SEM) and polarizing microscopy (PM). The <2 μm and 2 to 20 μm size fractions of sandstones and shales were separated by sedimentation and, together with the fracture fillings, analyzed by XRD, IRS, DTA and thermogravimetry (TGA).

A Siemens 501 diffractometer with CuKα radiation and graphite monochromator was operated at 35 mA, 40 kV, step size of 0.01°, and counting time of 1 s. Semiquantitative determination of the mineral composition was based on, either random powder mounts and the intensity factors of Shultz (1964), or oriented mounts on glass slides and the intensity factors of Islam and Lotse (1986). Routine treatment with ethylene glycol and dimethylsulfoxide, and heating at 550 °C to 650 °C for 2 h were systematically performed. Samples containing a kaolinite-type mineral were treated with potassium acetate and washed with water (KAc + H_2O) following the method of Wada (1965). Quantification of the nacrite content was based on the comparison of the intensity of the ≃7 Å reflections from the air-dried and

Table 1. Summary of lithology and mineralogical composition of cited samples.

Sample	Classification[1]	Medium size (mm)	Composition				
			Qz	Ab	C	D	Ph
1	Arkose	0.08	xxxx	xx	Tr	Tr	xx
2	Siltstone	0.04	xxx	xx	–	Tr	xxx
3	Greywacke	0.07	xxxx	x	xxx	–	xx
4	Feld. greywacke	0.06	xxx	xx	Tr	x	xxx
5	Siltstone	0.03	xxx	Tr	–	xx	xxx
6	Greywacke	0.20	xxxx	x	–	Tr	xxx
7	Greywacke	0.16	xxxx	x	–	x	xxx

[1] Classification: Pettijohn et al. (1972).

Abbreviations: Qz = Quartz; Ab = Albite; C = Calcite; D = Dolomite; Ph = Phyllosilicates; and Tr = In trace.

Mineral abundances: – = Not detectable; x = <10%; xx = 10–30%; xxx = 30–50%; and xxxx = >50%.

https://doi.org/10.1346/CCMN.1996.0440305 Published online by Cambridge University Press

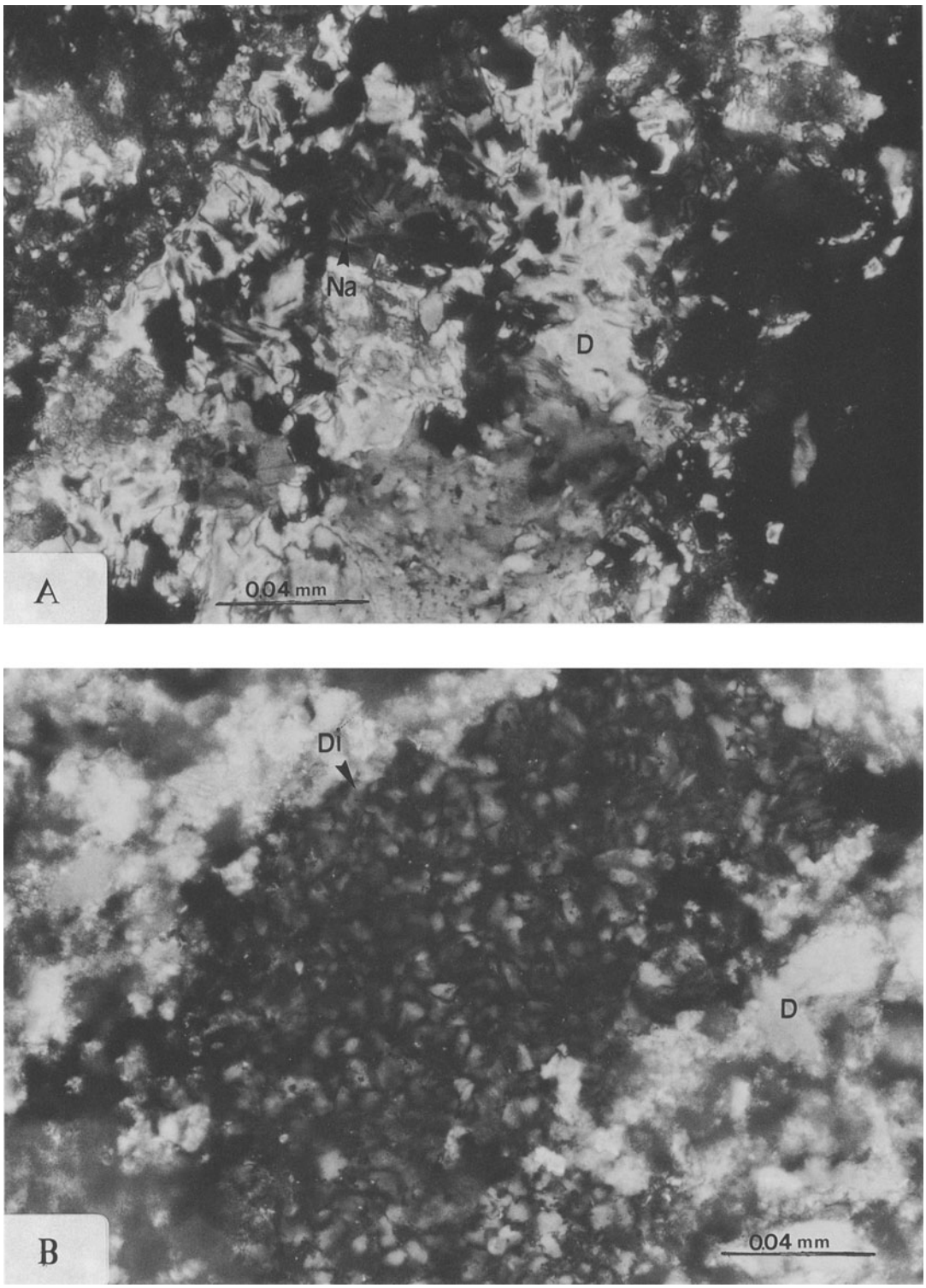

Figure 2. Photomicrographs of nacrite and dickite-rich veins. A) Intergrowths nacrite-dolomite. Sample 4. B) Dickite-rich vein. Sample 5. Polarizing filters crossed. Key: Na = nacrite; Di = Dickite; and D = dolomite.

https://doi.org/10.1346/CCMN.1996.0440305 Published online by Cambridge University Press

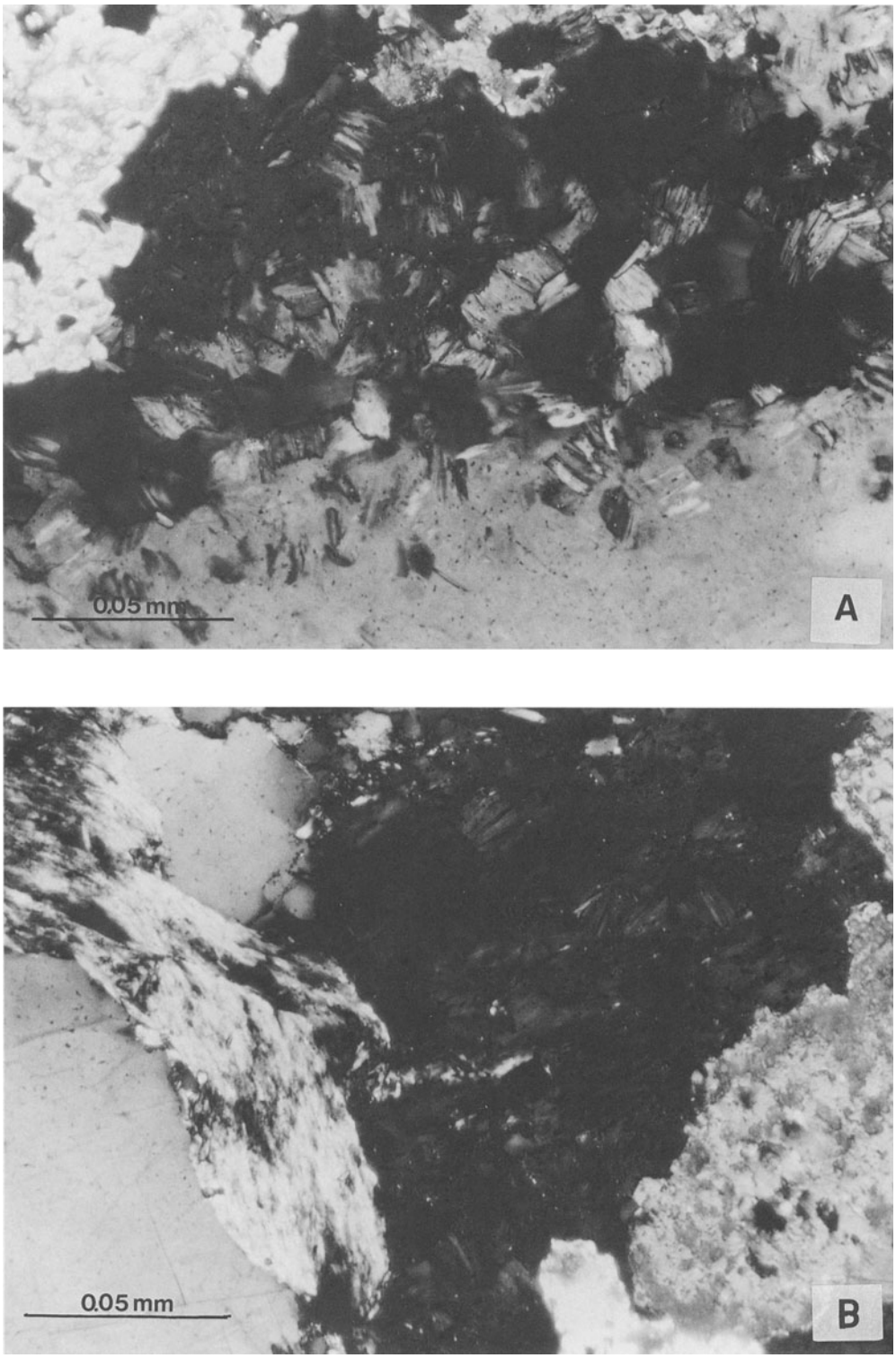

Figure 3. Photomicrographs of a nacrite-rich sandstone. Sample 6. A) Interstitial nacrite occurs as booklets of variable thickness, which locally replace quartz grains. B) Nacrite apparently formed from dissolution of large mica grains. Polarizing filters crossed.

https://doi.org/10.1346/CCMN.1996.0440305 Published online by Cambridge University Press

Table 2. Mineralogical composition of veins and 2–20 μm size fractions of sandstones and siltstones.

Sample	Composition								Na:Di + Int[1]	IC
	K	Il	Ch	ML	Qz	Ab	C	D		
1	xx	xx	–	–	xxx	xx	x	x	0:1	0.38
2	xx	xxx	–	x	xx	xx	–	–	n.d.	0.29
3	xxx	xx	–	x	xxx	x	x	–	1:1	0.35
4	x	xxx	xx	–	xxx	x	Tr	x	2:3	0.28
5	x	xxx	–	–	xxx	–	Tr	x	2:5	n.d.
6	xxx	xx	–	–	xx	x	–	x	4:1	0.32
7	xx	xxx	–	xx	xx	x	–	x	2:1	0.30
8[2]	xxx	x	–	–	xxx	–	–	x	6:1	n.d.
9[2]	xxxx	x	–	–	xx	–	–	–	1:10	n.d.
10[2]	xxx	x	–	–	xxxx	–	–	xx	1:3	n.d.
11[2]	xxxx	x	–	–	xxx	–	–	x	0:1	n.d.

[1] Deduced from the intensity of the 7 Å reflection after KAc + H_2O treatment.

[2] These samples belong to veins or fractures.

Abbreviations: K = kaolinite polytype; D = dickite, Na = nacrite; Int = intermediate phases; Il = illite; Ch = chlorite; ML = mixed-layer; Qz = quartz; Ab = albite; C = calcite; D = dolomite; and IC = illite crystallinity.

Mineral abundances: – = not detectable; x = <10%; xx = 10–30%; xxx = 30–50%; xxxx = >50%; and n.d. = not determined.

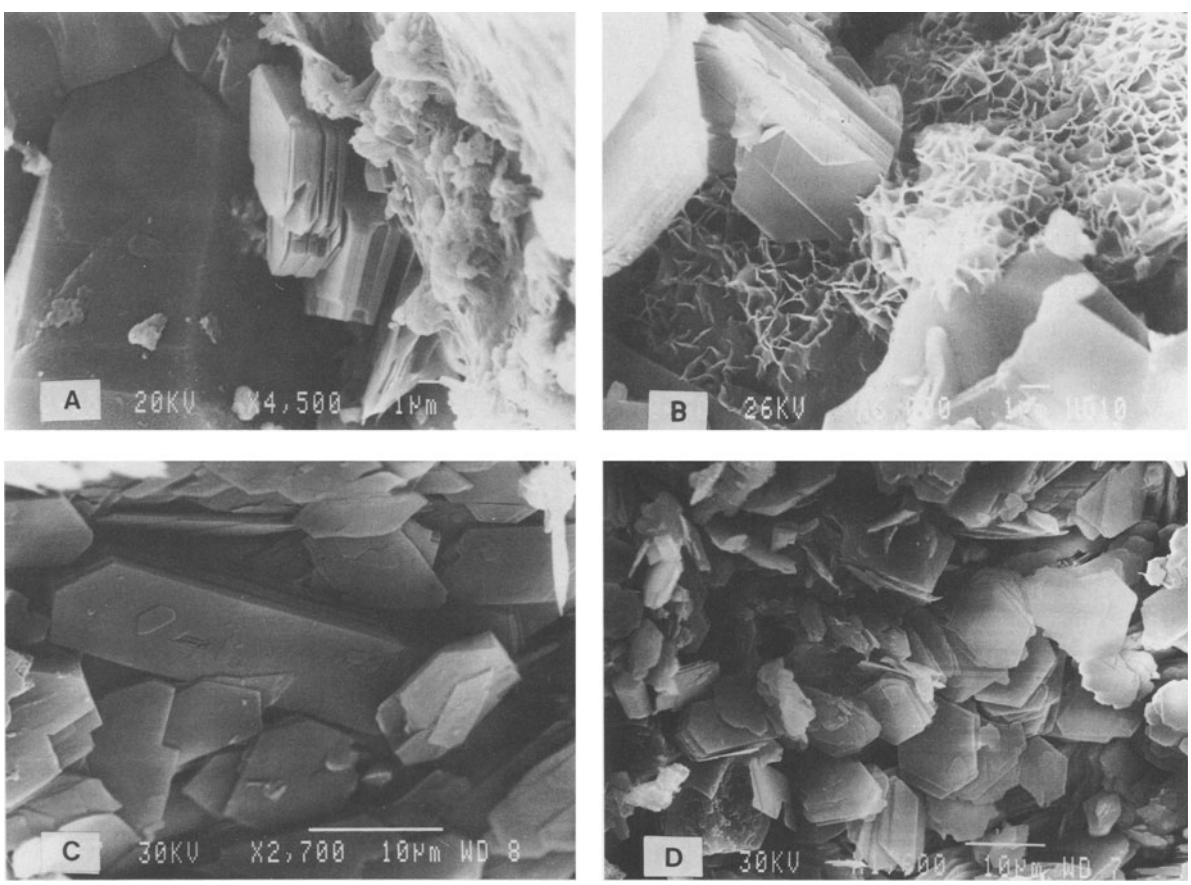

Figure 4. Scanning electron photomicrographs of nacrite. A) Photomicrograph showing the typical morphology of nacrite in sandstones. Sample 6. B) Textural relations between nacrite and mixed-layers containing chlorite, in sandstones. Sample 7. C) and D) Typical morphologies of nacrite in veins. Sample 8.

https://doi.org/10.1346/CCMN.1996.0440305 Published online by Cambridge University Press

the KAc + H_2O treated samples. Illite crystallinity (IC) was measured following the recommendations of Kisch (1991).

The morphologies and textural relations of the minerals were studied with a Leitz-Laborlux polarizing microscope and a Geol JSM-840 scanning electron microscope. SEM examination was on fractured surfaces of specimens after critical point drying and coating with gold.

Infrared spectra (IR) were recorded over the range 4000–240 cm^{-1} on a Perkin Elmer spectrophotometer, using KBr discs containing 2 wt.% of sample. The IR spectra obtained after heating at 60 °C showed a constant band at about 3400 cm^{-1} wide, generally ascribed to sorbed moisture (Farmer 1974). After drying the samples for 1 to 3 d at 105 °C and 200 °C these curves only showed slight modifications. Similar heating of an illite/mica rich sample resulted in spectra with a 3450 cm^{-1} wide band that can be ascribed to this mineral. Illite produced a fall in the base line in this zone of the IR spectra, thus making the correct estimation of the intensity of the several bands of these polytypes difficult.

Differential thermal analysis and DTG were carried out on a Rigaku-Thermoflex Tas 100 with samples of 35–40 mg, heated at 10 °C/min.

RESULTS

Nacrite has been identified filling very thin, irregular veins, associated with quartz and dolomite. For the most part, dickite fills distensive zones of fractures, either as the only component or accompanied by Fe-oxides and carbonates. Nacrite and dickite are also present within different sized sandstones and siltstones, which show the mineral assemblage of quartz-muscovite-kaolinite-type minerals, with or without albite, carbonates, chlorite and several types of mixed layer minerals containing chlorite. For shales, which showed the association quartz-albite-muscovite-chlorite, nacrite and dickite are hardly detectable. Tables 1 and 2 summarize the lithology and mineralogical composition of the samples cited.

Mixtures of dickite and nacrite have also been identified, but some of the studied samples show diffractograms that cannot be ascribed to dickite, nacrite or mixtures of both components. These occurrences appear to be similar to the "mixed-packets" of Shutov et al. (1970).

Microscopy

Thin sections of sandstones revealed nacrite, quartz and dolomite filling veins (Figure 2A) and as interstitial booklets frequently replacing quartz grains (Figure 3A). The clusters of nacrite were more common where large mica grains appear intensely dissolved (Figure 3B). In the veins, dickite formed clusters larger than nacrite, without visible quartz (Figure 2B).

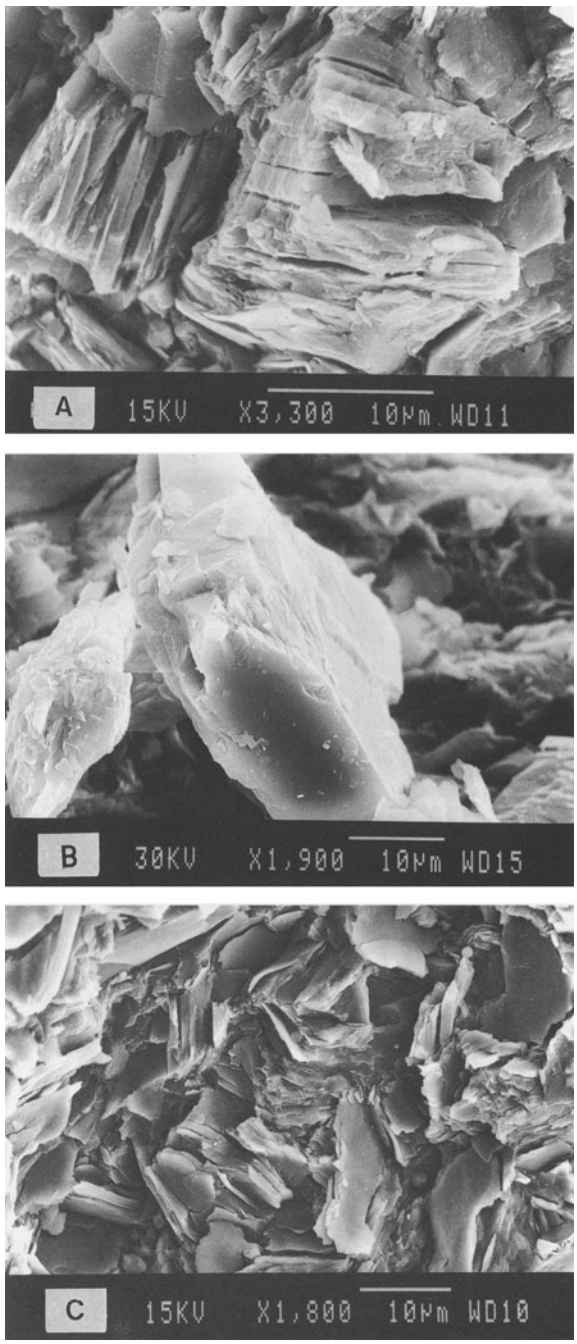

Figure 5. Scanning electron photomicrographs of dickite. Sample 9. A) Booklets of dickite with irregular forms. B) Thick crystal of dickite without apparent exfoliation. C) Stacks of dickite showing the irregular morphologies and sizes.

SEM examination of the sandstones showed blocky nacrite with pseudohexagonal morphology and crystal-sizes ranging from 10 to 20 μm (Figure 4A). In the veins, nacrite showed different forms. Booklets were

https://doi.org/10.1346/CCMN.1996.0440305 Published online by Cambridge University Press

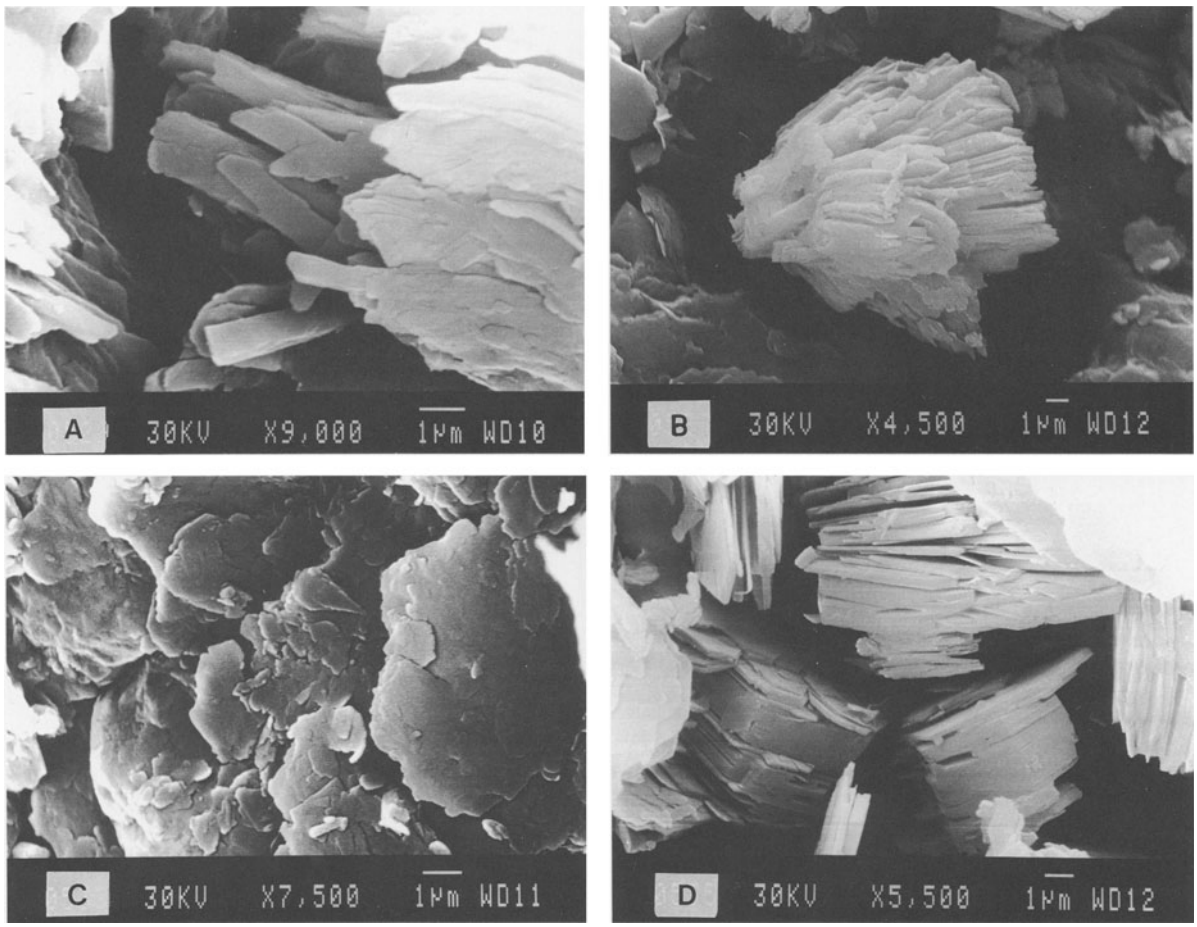

Figure 6. Scanning electron photomicrographs of possible mixed-layers. Sample 10. A) The thick, irregular aggregates of elongated plates are frequently shown by the intermediate phases. B) Booklets show rounded forms and appear formed by differently sized plates. C) This shows the most frequent morphologies and sizes of the mixed-layer aggregates. D) Booklets showing nacrite morphologies are found sporadically in these samples.

scarce and the large crystals (up to 30 μm long), elongated along the b-axis direction, predominated. Crystals have variable thickness and show well-defined, straight edges (Figure 4B, 4C and 4D). The crystal size was relatively uniform (≃10 μm) although smaller crystals in the order of 2 to 5 μm were also present. In contrast to nacrite, dickite veins showed thick crystals or plates with very irregular forms and variable particle size (Figure 5A, 5B and 5C). Intermediate phases showed variable morphologies and sizes. The more common aspect of these phases consisted of thick aggregates and booklets all with very irregular edges (Figure 6A, 6B and 6C), even though different morphologies were observed coexisting in the samples (Figure 6D).

X-ray Powder Diffraction

XRD patterns of different samples are shown in Figures 7, 8 and 9. Whereas dickite-rich samples contain scarce impurities, samples containing nacrite and intermediate phases offer a more complex mineralogy that makes the accurate identification of the reflections difficult (Table 3). The greatest differences among these diffractograms involve, as for kaolinites, the sequence of (20*l*) to (02*l*) and (31*l*) to (13*l*) reflections, in the ranges 19–28°, 34–42° and 45–57 °2θ. The indices of the nacrite structure or the position of the reflections (in Å) will be used to denote the reflections of the intermediate phases from the XRD.

In the range 19–29 °2θ (Figure 7), the dickite diffractogram agreed closely with the published data. Intensity ratios of the nacrite reflections were closer to data of Shutov et al. (1970) than to data of Bailey (1963). A weak reflection at 3.70 Å for both dickite and nacrite does not agree with any of the reported reflections of dickite or nacrite and could be due to the presence of some intermediate phases. These phases showed, in this range, variable diffractograms resembling that of slightly disordered kaolinites or dickites. The (11$\bar{1}$) reflection was enhanced relative to the (11$\bar{2}$) reflection. The reflections of both dickite and

https://doi.org/10.1346/CCMN.1996.0440305 Published online by Cambridge University Press

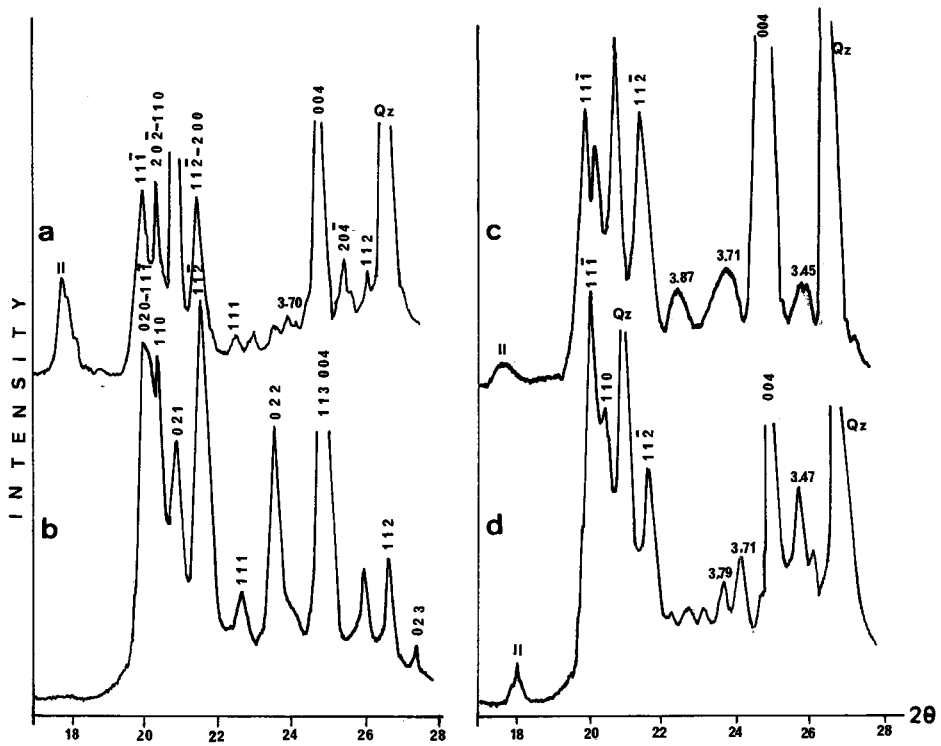

Figure 7. X-ray diffraction patterns in the range 18–28 °C (2θ). a) Nacrite-rich vein. Sample 8. b) Dickite-rich vein. Sample 9. c) and d) Possible mixed-layers-rich veins. Samples 10 and 11. Key: Qz = Quartz; and Il = Illite.

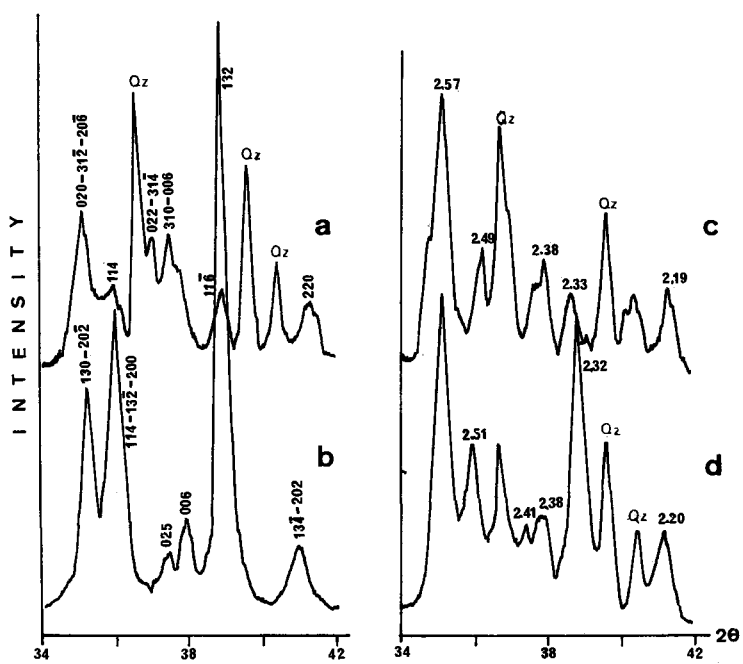

Figure 8. X-ray diffraction patterns in the range 34–42 °C (2θ). a) Nacrite-rich vein. Sample 8. b) Dickite-rich vein. Sample 9. c) and d) Possible mixed-layers-rich veins. Samples 10 and 11. Key: Qz = Quartz; and Il = Illite.

https://doi.org/10.1346/CCMN.1996.0440305 Published online by Cambridge University Press

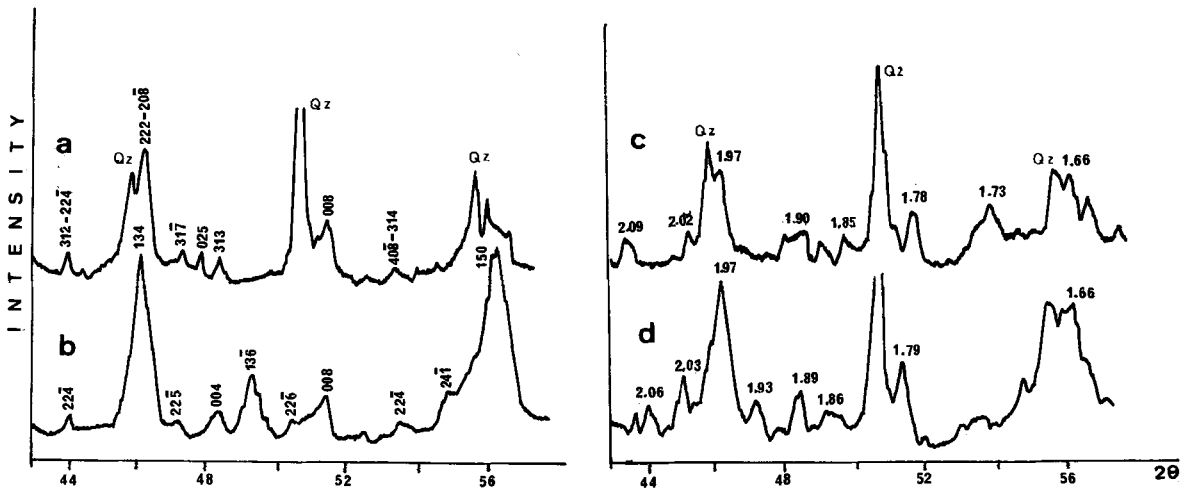

Figure 9. X-ray diffraction patterns in the range 45 to 57 °C (2θ). a) Nacrite-rich vein. Sample 8. b) Dickite-rich vein. Sample 9. c) and d) Possible mixed-layers-rich veins. Samples 10 and 11. Key: Qz = Quartz; and Il = Illite.

nacrite were present as well as irrational reflections (at 3.68 to 3.71 Å). The (20$\bar{4}$) reflection of nacrite showed an anomalous intensity compared to the nacrite diffractogram and frequently shifted between 3.49 and 3.45 Å. The possible influence of illite on the intensity of some reflections can be estimated from the (004) reflection of illite, which appears in Figure 7.

In the range 34 to 42 °2θ (Figure 8) the XRD of our dickite agreed with most of the published patterns. Our nacrite XRD showed the influence of illite on the en-

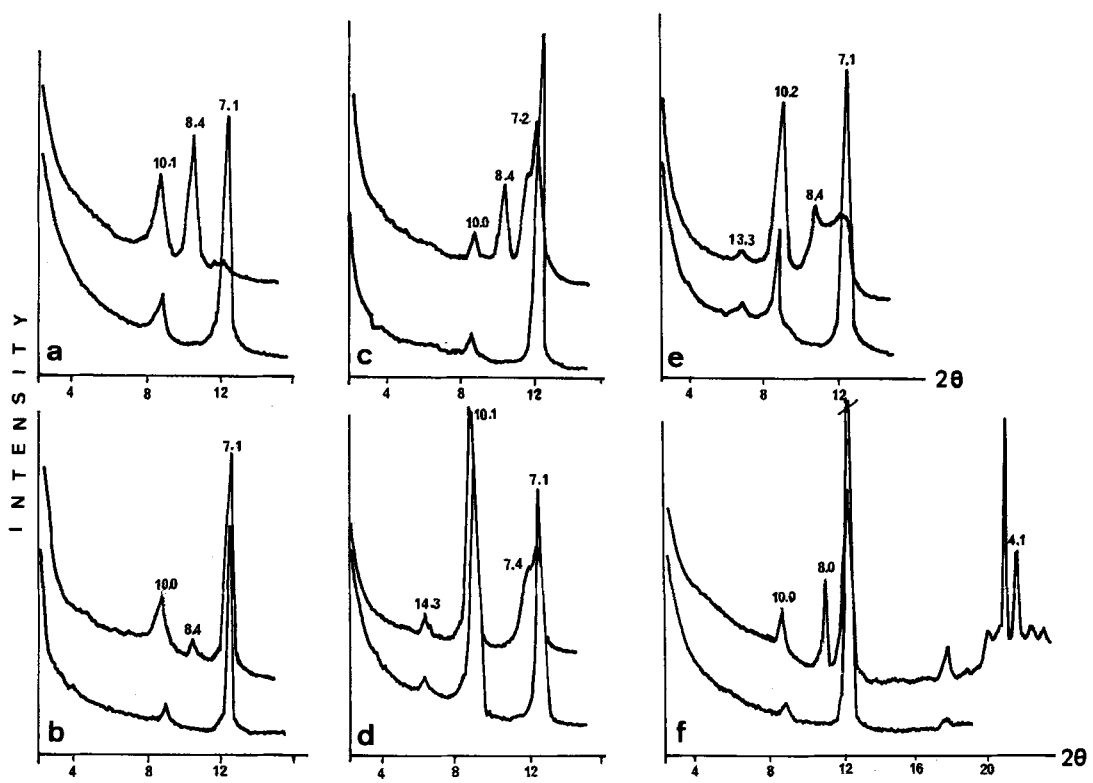

Figure 10. X-ray diffraction patterns after KAc + H_2O treatment. a) Nacrite-rich vein. Sample 8. b) Dickite-rich vein. Sample 9. c) Nacrite and intermediate phases. Sample 10. d) Dickite and intermediate phases. The 14.3 Å reflection belongs to tosudite. 2–20 μm size-fraction of sample 2. e) Nacrite and intermediate phases. The 13.3 Å reflection belongs to mica/chlorite mixed-layers. 2–20 μm size-fraction of sample 3. f) Dickite and intermediate phases. Sample 11.

https://doi.org/10.1346/CCMN.1996.0440305 Published online by Cambridge University Press

Table 3. X-ray powder data for dickite, nacrite and intermediate phases. Spacings in Å.

Dickite (sample 9)		Nacrite (sample 8)		Sample 10	
d	I	d	I	d	I
7.15	100	7.18	100	7.20	100
4.43	50	4.44	28	4.44	64
4.35	45	4.36	30	4.38	50
4.25	30				
4.12	60	4.13	30	4.13	41
3.95	15	3.93	10	3.94	<5
3.79	42			3.79	20
		3.63	<5	3.71	24
3.57	100	3.58	87	3.58	98
		3.47	20	3.47	22
3.43	20	3.41	16	3.41	18
3.25	8				
		3.11	8	3.11	8
3.09	8	3.06	14	3.06	8
2.93	8	2.92	†		
2.79	8			2.78	14
2.65	6	2.68	†		
2.56	35	2.56	†	2.57	†
		2.54	20		
2.51	47	2.51	10	2.51	33
		2.43	22		
2.41	10	2.40	†	2.41	†
2.38	17			2.38	†
2.32	85	2.32	15	2.32	48
		2.28	†		
		2.24	†		
2.21	13	2.19	14	2.20	23
		2.11	†		
2.05	5	2.07	8	2.08B	10
		2.03	†	2.03	†
		1.99	†		
1.97	28	1.97	†	1.97	†
1.93	<5	1.93	8	1.93	8
		1.91	8		
1.89	10	1.89	7	1.89	13
1.86	12			1.86	10
1.80	<5				
1.79	9	1.79	13	1.79	20
1.76	<5	1.77	5		
1.71	<5	1.73	5	1.72B	8
1.69	8	1.68	†		
1.650	30	1.655	13	1.660	24
1.611	<5	1.616	5	1.621	<5
1.587	<5				
1.555	15	1.553	7		
1.488	30	1.486	18	1.486	28
		1.473	<5	1.469	12

† Overlap with quartz, albite, dolomite or illite reflections. B = Band.

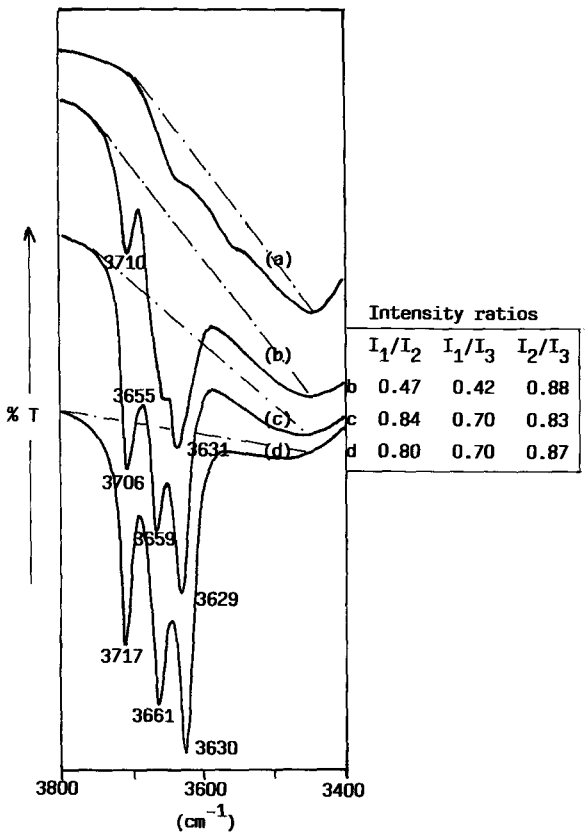

Figure 11. Infrared spectra in the hydroxyl-stretching bands region and intensity ratio of the three bands (1: 3700 cm^{-1}; 2: 3650 cm^{-1}; 3: 3630 cm^{-1}). a) Illite-rich sample. b) Nacrite-rich vein. Sample 8. c) Possible mixed-layers-rich vein. Sample 10. d) Dickite-rich vein. Sample 9. Dashed lines indicate the theoretical base-line, subtracting the influence of the illite.

hancement of the 2.56 Å reflection. An anomalous reflection at 2.19 Å is probably due to an intermediate phase. In the diffractogram, the intensities of the reflections at 2.50 Å and 2.32 Å agreed with a "mixture" of nacrite and dickite. Nevertheless, while a variable shift of the reflection at 2.32 Å and an enhancement of the 2.19 Å and 2.56 Å reflections at the same time, this cannot be justified by the presence of illite.

In the range 45° to 57 °2θ (Figure 9) the intermediate phase again showed reflections of both dickite and nacrite, together with some reflections that cannot be explained by a mixture of both components. For example, the reflections at 2.02 Å and 1.78 Å were remarkably enhanced, and the reflection at 1.88 Å was enhanced and/or shifted.

The treatment of Wada (1965) confirms the diverse composition of the samples (Figure 10). While nacrite-rich and dickite-rich samples produce well-defined peaks at 8.4 and 7.1 Å (Figure 10A and 10B), a variety of effects appear from samples containing mixtures and/or intermediate phases. The more common features consist of: the shift of the 7.1 Å reflection (Figure 10C); the presence of a shoulder at 7.4 to 7.5 Å for the dickite reflection (Figure 10C and 10D); and less frequently, the presence of a band between 7.1 and 8.4 Å (Figure 10F) or a well-defined effect at 7.9 to 8.0 Å (Figure 10E). Simultaneously, the frequent enhancement and shift of the 10 Å reflection after the treatment indicates the presence of a complex superimposed on the illite reflection.

https://doi.org/10.1346/CCMN.1996.0440305 Published online by Cambridge University Press

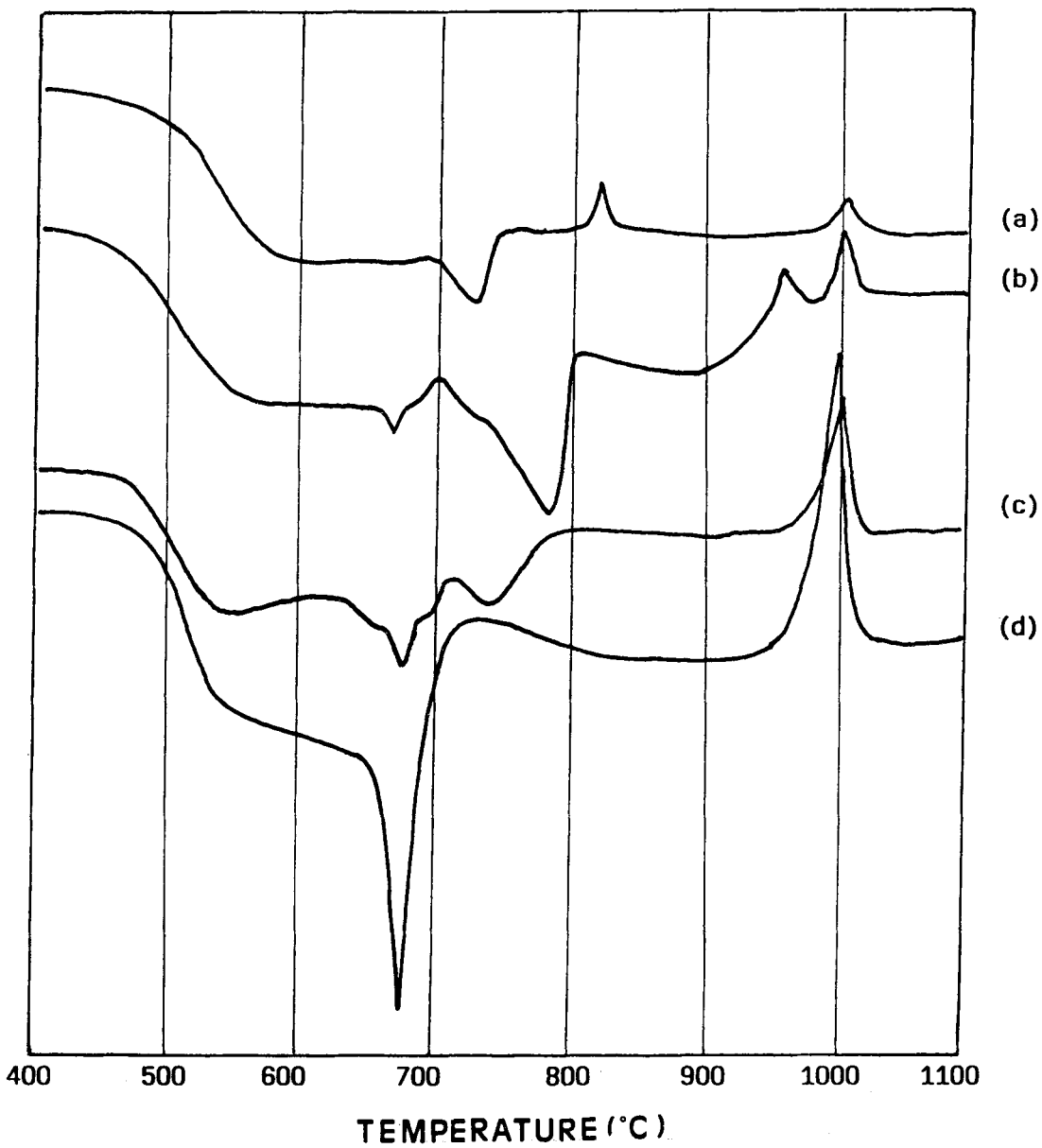

Figure 12. Differential thermal analysis of a) 2–20 μm size-fraction of sample 6. b) Nacrite-rich vein. Sample 8. c) Possible mixed-layer-rich vein. Sample 10. d) Dickite-rich vein. Sample 9.

Infrared Spectra

IR spectra of dickite-rich samples showed the absorption bands expected for a well-ordered mineral (Figure 11D). Although, they appear slightly shifted toward higher frequencies in relation to the values commonly cited. IR spectra of nacrite-rich samples showed a weak band at 3710 cm^{-1} and two medium-strong bands at 3655 and 3631 cm^{-1} (Figure 11B). Our spectrum compared to that of Hanson et al. (1981) for hydrothermal nacrite showed a shift of the intermediate frequency band toward the dickite position and decreased intensity as can be deduced from the intensities ratios presented in Figure 11. The intermediate phases showed spectra in which the "mixed" composition was revealed by the intensity of the low frequency band. This band appeared shifted, toward low frequencies and the 3659 cm^{-1} band weakened in relation to the dickite and nacrite spectra. The presence of muscovite caused a considerable slope and deviation from the ideal base line for all the spectra. Because of this, the intensity ratios have been calculated from the sloped "base lines" drawn on the spectra.

https://doi.org/10.1346/CCMN.1996.0440305 Published online by Cambridge University Press

Thermal Analyses

The DTA curves of dickite-rich samples (Figure 12d) showed the main endothermic effect at 680 °C and the main exothermic effect at 980 °C. They are very similar to DTA curves for well-ordered dickites compiled by Brindley and Porter (1978). Nacrite and intermediate phases showed weaker thermal effects than dickite due to the high quartz content of these samples (about 30%). In addition, the curves were more complex due to the presence of carbonates (Figure 12a, 12b and 12c). Curve a was the most characteristic of nacrite-rich samples, in which the carbonate content was <5%. Curve b belongs to a nacrite-rich sample with higher carbonate content (10%). For this curve, the position of the main endothermic effect resembled that of ankerite (Mackenzie 1970), but the microprobe analyses indicated a composition $(Ca_{0.5}Mg_{0.4}Fe_{0.1})CO_3$, which does not agree with the endothermic position. The intermediate phases (Figure 12c) showed intermediate curves between those of nacrite and dickite, but with a marked endothermic effect at 540 °C and a single exothermic effect at 1000 °C.

XRD patterns of the nacrite-rich samples heated at 750 °C showed the β-quartz reflections and the disappearance of the nacrite reflections and a wide band (5 to 2.9 Å) of very disordered phases. The heating at 850 °C resulted in an increase of the quartz ratio and the decrease of the "amorphous" band, which showed two weak maxima at about 3.4 and 4.4 Å. This behavior suggests that the 830 °C exothermic effect can be related to the reorganization of the silica tetrahedra and the formation of β-quartz.

DISCUSSION

IR spectrum of nacrite showed some differences in relation to the available data for this mineral, which mainly affected the 3655 cm^{-1} band. The assignment of this band to kaolinite, dickite and nacrite is still controversial. Differences in orientation of the OH bonds of the surface hydroxyls and consequently, differences in the intensity of hydrogen bonding have been used frequently to explain this band (Rouxhet et al. 1977) and the observed differences between IR spectra of the three polytypes. Nevertheless, after the recent refinements of the crystal structures of kaolinite, dickite and nacrite (Suitch and Young 1983; Zheng and Bailey 1994), this explanation seems to be inconsistent since the three surface hydroxyls show similar orientations. Thus, the similarity shown by dickite and nacrite for this zone of the spectra appears to be reasonable. Nevertheless, the position and intensity of the highest frequency band showed remarkable differences between dickite and nacrite, which agree with the values commonly observed for these polytypes.

As a consequence of the similarity in the position of the dickite and nacrite IR bands, the differences that can be manifested for the spectrum of the intermediate phases are scarce and affect only the highest frequency band. The intensity of this band is clearly greater than that expected from a mixture of both polytypes and simultaneously, it appears affected by a shift toward low frequency values. These data suggest that for this intermediate phase the surface hydroxyls are in specific configurations on the molecular scale, as suggested by Prost et al. (1989) for disordered kaolinites showing anomalous bands.

DTA curves of nacrite (Figure 12a and 12b) indicate an anomalous thermic behavior as compared to the few published DTA curves of this polytype although the presence of dolomite prevents the accurate characterization of nacrite by DTA. The exothermic effect at 830 °C may be interpreted as a structural reorganization of the silica tetrahedra which would be the beginning of a very ordered nacrite structure. Since the DTA curve of nacrite cannot be clearly interpreted, little additional information about the composition or structure of the intermediate phases can be obtained from the DTA curves. However, they far resemble nacrite in the 680 to 720 °C endothermic effects, dickite from the position and intensity of the exothermic effect, and disordered kaolinites or dickites for the enhancement of the 540 °C endothermic effect.

XRD patterns of nacrite shown in Figures 7, 8 and 9 exemplify a well-ordered mineral. However, they show some differences compared to data published by Bailey (1963) in terms of intensities of some non-basal reflections. The published data concerning hydrothermal nacrites indicate for this mineral a high degree of crystallinity. The available data about finely grained nacrites (<1 μm) of authigenic origin also indicate a high degree of crystallinity (Bühmann 1988). This agreement between nacrites with different origins and particle sizes can, in principle, lead one to think that all nacrites are structurally well-ordered and morphologically well-formed (Brindley 1980). Nevertheless, it is reasonable to suspect that nacrite can show, as kaolinite and dickite, some type of disorder. The intermediate phases could be considered either as disordered phases, as well as dickite/nacrite mixed-layers. The characteristics of the diffractogram from the 19–22 °2θ range suggests a certain increasing disorder as compared with the patterns of dickite or nacrite. By analogy with kaolinite, this behavior could indicate the presence of translation defects, or more probably, of mixtures of two phases with a different degree of ordering, thus following the idea by Plançon and Zacharie (1990). Disorder within kaolinites and dickites is clearly reflected by the XRD patterns by the weakening of some well-defined reflections (k = 3n), while for our samples, some reflections with k = 3n (3.70 Å, 3.48 Å, 2.09 Å) appear enhanced and frequently shifted. Thus, although the presence of mixtures in these samples is evident from the SEM examination,

https://doi.org/10.1346/CCMN.1996.0440305 Published online by Cambridge University Press

the behavior of the hkl reflections point out the presence of mixed-layers of intermediate composition, according to the results by Shutov et al. (1970).

The KAc + H_2O test also confirms the presence of mixtures and phases with anomalous behavior. The 10 Å complex is typical of halloysite, but this mineral has not been identified by DTA, XRD or microscopy. Consequently, this 10 to 10.3 Å complex can be ascribed to intermediate phases together with the effects at 7.4 to 7.5 and 7.9 to 8.0 Å. These data are not conclusive, but point to a certain specificity and regularity for the structural configuration of these phases.

From a genetic point of view, nacrite formation within Paleozoic materials can be related to prograde metamorphism. Zonation is simultaneously marked by the IC values and the presence of kaolinite, dickite and nacrite from Permo-Triassic to Carboniferous materials. This evolution is to a great extent similar to that showed by Shutov et al. (1970). The metamorphic conditions in which nacrite has been developed belong to anchizone, as can be deduced from the IC values for fine-grained rocks (Kisch 1990).

Microscopic examination shows that interstitial nacrite is preferently developed near partially dissolved mica grains. Therefore, it seems likely that nacrite has been formed directly from these. The euhedral morphologies shown by the nacrite crystals also point to direct crystallization from solutions. Because of this, and in spite of the attractive interpretation given by Shutov et al. (1970), that supposes the dickite → nacrite transformation through mixed-packets dickite/nacrite, the genetic relation between dickite and nacrite is still not clear for our samples and a more detailed study will be carried out.

REFERENCES

Bailey SW. 1963. Polymorphism of the kaolin minerals. Am Miner 48:1196–1209.

Bourgois J. 1978. La transversale de Ronda (Cordillères Bétiques, Espagne). Donnés géologiques pour un modele d'évolution de l'arc de Gibraltar. Ann Sci Univ Besançon Géol 3ème série 30:445p.

Brindley GW. 1980. Order-disorder in clay mineral structures. In: Brindley GW, Brown G, editors. Crystal structures of clay minerals and their X-ray identification. London: Mineralogical Society. 125–195.

Brindley GW, Porter ARD. 1978. Occurrence of dickite in Jamaica. Ordered and disordered varieties. Am Mineral 63: 554–562.

Bühmann D. 1988. An occurrence of authigenic nacrite. Clays & Clay Miner 36:137–140.

Deer VA, Howie RA, Zussman J. 1976. Rock-forming minerals. Vol. 3: Sheet silicates. London: Longman. 270 p.

Dunoyer de Segonzac G. 1970. The transformation of clay minerals during diagenesis and low-grade metamorphism: A review. Sedimentol 15:281–326.

Farmer VC. 1974. The infrared spectra of minerals. London: Mineralogical Society. 539 p.

Felder TE. 1978. Zur geologischen Entwicklung der Betischen Internzonen der westlichen Serranía de Ronda (Prov. Málaga, Spanien). Zurich:Mitt Geol Inst ETH. 222:168 p.

Ferrero J, Kubler B. 1964. Presence de dickite et de kaolinite dans les grès Cambriennes d'Hassi Massaoud. Bull Serv Carte Geol Als Lorr 17:247–261.

Frey M. 1987. Very low-grade metamorphism of clastic sedimentary rocks. In: Frey M, editor. Low temperature metamorphism. Glasgow and London: Blackie. 9–58.

Hanson RF, Zamora R, Keller WD. 1981. Nacrite, dickite and kaolinite in one deposit in Nayarit, Mexico. Clays & Clay Miner 29:451–453.

Islam AKME, Lotse EG. 1986. Quantitative mineralogical analysis of some Bangladesh soils with X-ray, ion exchange and selective dissolution techniques. Clay Miner 21:31–42.

Kisch HJ. 1990. Calibration of the ankizone: A critical comparison of illite crystallinity scales used for definition. J Metamorphic Geol 8:31–46.

Kisch HJ. 1991. Illite crystallinity: Recommendations on sample preparation, X-ray diffraction settings, and interlaboratory samples. J metamorphic Geol 9:665–670.

Mackenzie RC. 1970. Simple phyllosilicates based on gibbsite and brucite-like sheets. In: Mackenzie RC, editor. Differential thermal analysis. London: Academic Press. p 498–537.

Mäkel GG. 1985. The Geology of the Malaguide Complex and its bearing on the Geodynamic evolution of the Betic-Rif orogen (Southern Spain and northern Marocco). Gua Papers of Geology. 22:263 p.

Plançon A, Zacharie C. 1990. An expert system for the structural characterization of kaolinites. Clay Miner 25:249–260.

Prost R, Dameme A, Huard E, Driard J, Leydecker JP. 1989. Infrared study of structural OH in kaolinite, dickite, nacrite and poorly crystalline kaolinite at 5 to 600 K. Clays & Clay Miner 37:464–468.

Rouxhet PG, Samadacheata N, Jacobs H, Anton O. 1977. Attribution of the OH stretching bands of kaolinite. Clay Miner 12:171–178.

Ruiz Cruz MD, Moreno Real L. 1993. Diagenetic kaolinite/dickite (Betic Cordilleras, Spain). Clays & Clay Miner 41:570–579.

Ruiz Cruz MD. 1996a. Genesis and transformation of dickite in Permo-Triassic sediments (Betic Cordilleras, Spain). Clay Miner 31:133–152.

Ruiz Cruz MD. 1996b. Criterios mineralógicos utilitados en el análisis del Permotrías Maláguide. Cuad Geol Ibérica 20: 37–59.

Russell JD. 1987. Infrared methods. In: Wilson JM, editor. A handbook of determinative methods in clay mineralogy. Glasgow: Blackie. 133–173.

Shen ZY, Wilson MJ, Fraser AR, Pearson MJ. 1994. Nacritic clay associated with the Jiangshan—Shaoxing deep fault in Zhejiang province, China. Clays & Clay Miner 42:576–581.

Shultz LG. 1964. Quantitative interpretation of mineralogical composition from X-ray and chemical data for the Pierre Shale. U.S. Geol Surv Prof Paper 391-C:31p.

Shutov VD, Aleksandrova AV, Losievskaya SA. 1970. Genetic interpretation of the polymorphism of the kaolinite group in sedimentary rocks. Sedimentol 15:69–82.

Suitch PR, Young RA. 1983. Atom positions in highly ordered kaolinite. Clays & Clay Miner 31:357–366.

Van der Marel HW, Beutelspacher H. 1976. Atlas of infrared spectroscopy of clay minerals and their admixtures. Amsterdam: Elsevier. 396 p.

Wada K. 1965. Intercalation of water in kaolin minerals. Am Mineral 50:924–941.

Wilson MJ. 1987. X-ray diffractions. In: Wilson JM, editor. A handbook of determinative methods in clay mineralogy. Glasgow: Blackie. 26–98.

Zheng H, Bailey SW. 1994. Refinement of the nacrite structure. Clays & Clay Miner 42:46–52.

(Received 20 January 1995; accepted 3 August 1995; Ms. 2610)